X-ray diffraction study of surface acoustic waves and pseudo-surface acoustic waves propagation in La3Ga5.5Ta0.5O14 crystal

Dmitry Roshchupkin, Luc Ortega, Olga Plotitcyna, Alexei Erko, Ivo Zizak, and Dmitry Irzhak

---

Articles you may be interested in

X-ray diffraction on the X-cut of a Ca3TaGa3Si2O14 single crystal modulated by a surface acoustic wave
J. Appl. Phys. **115**, 244903 (2014); 10.1063/1.4884875

X-ray imaging of the surface acoustic wave propagation in La3Ga5SiO14 crystal
Appl. Phys. Lett. **103**, 154101 (2013); 10.1063/1.4824127

Piezoelectric strain coefficients in La3Ga5.3Ta0.5Al0.2O14 and Ca3TaGa3Si2O14 crystals
AIP Advances **3**, 102108 (2013); 10.1063/1.4824636

Diffraction of a focused x-ray beam from La3Ga5SiO14 crystal modulated by surface acoustic waves
J. Appl. Phys. **110**, 124902 (2011); 10.1063/1.3669399

X-ray Bragg diffraction from langasite crystal modulated by surface acoustic wave
J. Appl. Phys. **94**, 6692 (2003); 10.1063/1.1619199

X-ray diffraction study of surface acoustic waves and pseudo-surface acoustic waves propagation in La$_3$Ga$_{5.5}$Ta$_{0.5}$O$_{14}$ crystal

Dmitry Roshchupkin,[1,a)] Luc Ortega,[2] Olga Plotitcyna,[1] Alexei Erko,[3] Ivo Zizak,[3] and Dmitry Irzhak[1]

[1]*Institute of Microelectronics Technology and High-Purity Materials Russian Academy of Sciences, Chernogolovka, Moscow District 142432, Russia*
[2]*Laboratoire de Physique des Solides, Univ. Paris-Sud, CNRS, UMR 8502, F-91405 Orsay Cedex, France*
[3]*Institute for Nanometre Optics and Technology, Helmholtz-Zentrum Berlin für Materialien und Energie GmbH, Albert-Einstein Strasse 15, 12489 Berlin, Germany*

X-ray diffraction on the crystal La$_3$Ga$_{5.5}$Ta$_{0.5}$O$_{14}$ modulated by surface acoustic waves (SAW) and pseudo-surface acoustic waves (PSAW) with wavelength of $\Lambda = 8$ μm was studied using a double axis X-ray diffractometer at the BESSY II synchrotron radiation source. The propagation of SAW and PSAW leads to sinusoidal modulation of the crystal lattice and gives rise to diffraction satellites on the rocking curve, with the intensity and angular divergence between the diffraction satellites depending on the wavelength and amplitude of the crystal lattice acoustic modulation. The analysis of diffraction spectra enables the determination of the amplitude and acoustic wavelengths, and power flow angles of acoustic energy propagation. The investigation of acoustic wave fields showed that PSAW is a flowing back wave which propagates at an angle to the crystal surface. © *2013 AIP Publishing LLC*. [http://dx.doi.org/10.1063/1.4801527]

I. INTRODUCTION

Acoustoelectronic devices based on surface acoustic waves (SAW) are widely used in telecommunication systems for information processing and data transfer. Such devices are also efficient in sensor devices, wireless ones included. In recent years, novel piezoelectric materials promising for acoustoelectronics have been extensively searched. Much attention has been given to crystals of lanthanum-gallium silicate group, which possess both good piezoelectric and thermal properties.[1–4] Note that SAW velocities in these crystals are small, which makes the crystals attractive for the fabrication of miniature acoustoelectronic devices.

Methods of X-ray topography and diffraction are of special interest in the studies of the crystal acoustic properties because they enable the visualization of acoustic wave fields in the crystals in the on-line mode. The X-ray topography method used in the region of Fresnel diffraction provides the visualization of acoustic wave fields on the crystal surface.[5–10] The acoustic wave fields were visualized in the main acoustic cuts of the langasite La$_3$Ga$_5$SiO$_{14}$ crystal, and power flow angles were measured by X-ray topography, because in this crystal the direction of the SAW wave vector does not coincide with the direction of the power flow vector.[9] The SAW propagation in the crystals can also be studied by X-ray diffraction which permits the SAW amplitude to be measured by the analysis of the diffraction spectra. Surface acoustic wave propagation causes sinusoidal modulation of the crystal lattice and leads to the appearance of diffraction satellites on the rocking curve.[11–13] The intensity of satellites is determined by the acoustic wave amplitude, and the angular divergence between the satellites is determined

by the SAW wavelength. X-ray diffraction was used to study the SAW propagation in the $Y-$ and $X-$cuts of La$_3$Ga$_5$SiO$_{14}$ and La$_3$Ga$_{5.5}$Ta$_{0.5}$O$_{14}$ crystals, which allowed us to measure the SAW amplitude and power flow angles.[14–16] X-ray diffraction was employed to test a high-temperature sensor device based on SAW, fabricated on the basis of the La$_3$Ga$_5$SiO$_{14}$ crystal.[17]

The aim of this work was to study the pseudo-surface acoustic waves (PSAW) excitation and propagation in the La$_3$Ga$_{5.5}$Ta$_{0.5}$O$_{14}$ (LGT) crystal. PSAWs are now an interesting object of investigation because PSAW, like SAW, can be excited using an interdigital transducer (IDT). SAW and PSAW have the same wavelength but different velocities and, consequently, are excited at different frequencies. In this work, the double axis X-ray diffractometer was used to study SAW and PSAW excitation and propagation in the $Z-$cut of the LGT crystal and to measure the power flow angles.

II. EXPERIMENTAL SETUP

Figure 1 displays the schematic drawing of a double axis X-ray diffractometer setup on the KMC2 optical beamline at the BESSY II synchrotron radiation source. The energy of X-ray radiation near the $K-$edge of Ga was $E = 11$ keV, which corresponds to kinematical diffraction. The energy was selected with a Si(111) double-crystal monochromator, and X-ray radiation was collimated with a 60×60 μm^2 entrance slit. The incident angle of X-ray radiation was the Bragg angle. Acoustic modulation of the crystal lattice gives rise to diffraction satellites on the rocking curve with the angular divergence between the satellites

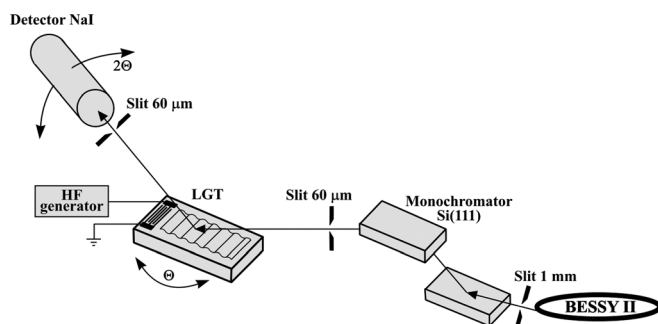$$\delta\Theta = d/\Lambda, \qquad (1)$$

a)Electronic mail: rochtch@iptm.ru

113, 144909-1

FIG. 1. Experimental setup.

where d is the interplanar spacing, and Λ is the acoustic wavelength. The angular divergence between the diffraction satellites is determined from Eq. (1) and the intensity of diffraction satellites depends on the amplitude of the crystal lattice acoustic vibrations.[11–16] A standard NaI scintillation detector with a 60 μm entrance slit was used to recorder the diffracted X-ray intensity.

III. SAW DEVICE

LGT is a piezoelectric crystal of the point group symmetry 32. The crystal unit cell parameters are $a = 8.235$ Å and $c = 5.125$ Å.[18] The crystal was grown along the {110} axis by the Czochralski method at the FOMOS Materials Co.

The $Z-$cut of the LGT crystal (the (001) planes are parallel to the crystal surface) was used to study the SAW and PSAW propagation. On the crystal surface, an IDT was formed by photolithography technique to excite the SAW and PSAW. The IDT was formed on the crystal surface so that the wave vector of the acoustic wave is along the $(X + 30°)$ direction. The IDT consisted of 50 pairs of metallic electrodes with a 4 μm period, which corresponds to the SAW wavelength of $\Lambda = 8$ μm. The acoustic wave amplitude could be varied linearly from zero to several angstroms by changing the amplitude of the input high-frequency signal supplied to the IDT. At the resonance frequency $f = 320$ MHz, the IDT excites the SAW which propagates with the velocity $V = 2560$ m/s, and at the resonance frequency $f = 360$ MHz the PSAW is excited with the velocity $V = 2880$ m/s. The propagation of SAW and PSAW in the $Z-$cut of the LGT crystal is characterized by the power flow angle, i.e., the direction of power flow vector (PFV) does not coincide with the direction of the acoustic wave vector.

IV. EXPERIMENTAL RESULTS

To study the SAW and PSAW propagation in the $Z-$cut of the LGT crystal along the $(X + 30°)$ direction at various acoustic amplitudes, rocking curves were measured at X-ray energy $E = 11$ keV (X-ray wavelength $\lambda = 1.17$ Å). The reflection from the (001) planes at the Bragg angle $\Theta_B = 6.595°$ was used in the experiment.

Figure 2 shows the map of acoustic wave field distribution of SAW (a) and PSAW (b) on the $Z-$cut surface of LGT. The data were obtained at the amplitude of the input signal on an IDT $U = 15$ V and present the distribution of X-ray intensity on the crystal surface, which was diffracted
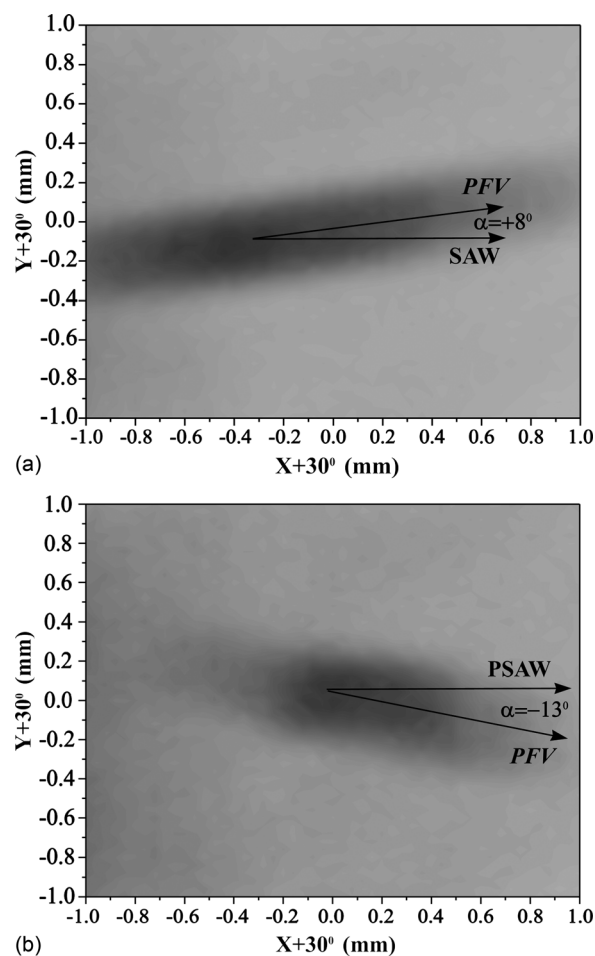

FIG. 2. Maps of the diffracted X-ray intensity: (a) SAW, (b) PSAW. $E = 11$ keV; reflection (001); $\Theta_B = 6.595°$; $\Lambda = 8$ μm. Dark contrast corresponds to the SAW (PSAW) propagation.

to the first diffraction satellite. It is clearly seen from the maps that the direction of the SAW and PSAW wave vectors does not coincide with the PFV direction, i.e., the power flow angle occurs. Moreover, SAW and PSAW propagation differ by the direction and signs of the power flow angle. For SAW the power flow angle is $\alpha = +8°$, for PSAW it is $\alpha = -13°$. It is also seen in the figure that the PSAW acoustic wave field on the $Z-$cut surface of LGT can be observed only near the IDT, whereas the SAW acoustic wave field can be observed on the whole surface of the piezoelectric substrate. This means that PSAW is a flowing-back wave which propagates from the IDT into the crystal depth at an angle to the crystal surface. X-ray diffraction on the PSAW-modulated crystal can be observed only near the IDT.

Figure 3 displays the rocking curves of the $Z-$cut of LGT crystal modulated by the SAW (a) and PSAW (b) with the wavelength $\Lambda = 8$ μm. The rocking curves were measured at the amplitude of the input signal on an IDT $U = 15$ V. The angular divergence between the diffraction satellites on the rocking curve is $\delta\Theta \approx 0.005°$, which corresponds to the value calculated from Eq. (1) for the acoustic wavelength $\Lambda = 8$ μm. This similar divergence between diffraction satellites in the cases of SAW and PSAW suggests that these wave processes have similar wavelengths. As can be seen from Fig. 3, the rocking curves of the $Z-$cut of LGT crystal
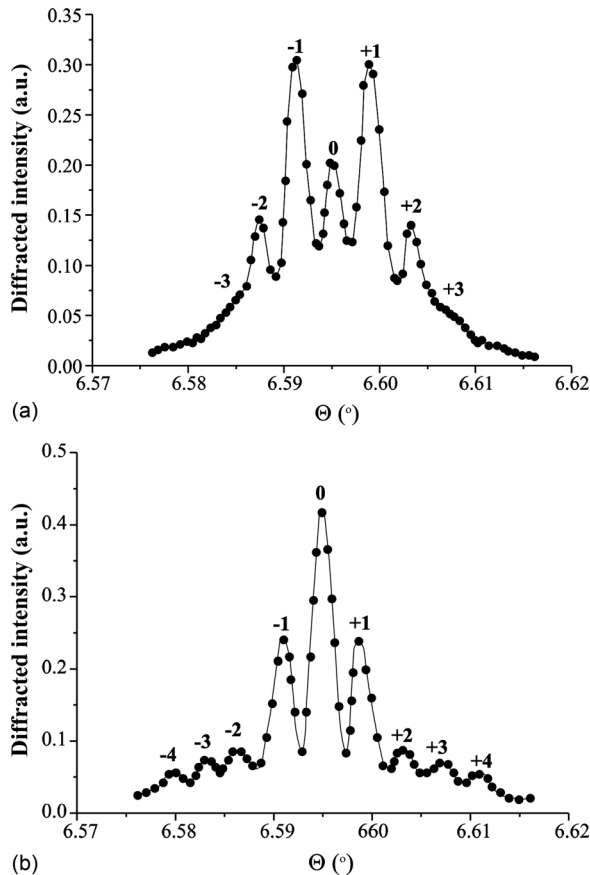
FIG. 3. Rocking curves of the $Z-$cut of an LGT measured for SAW (a) and PSAW (b). $E = 11$ keV; reflection (001); $\Theta_B = 6.595°$; $\Lambda = 8$ μm.

FIG. 4. Intensities of the diffraction satellites ($m = 0, 1, 2$) in the $Z-$cut of an LGT vs. amplitude of the input signal supplied to the IDT U: (a) SAW; (b) PSAW. $E = 11$ keV; reflection (001); $\Theta_B = 6.595°$; $\Lambda = 8$ μm.

modulated by SAW and PSAW differ from each other. In the case of SAW modulation, the diffraction is kinematic at the X-ray energy $E = 11$ keV and the intensities of diffraction satellites are described by the Bessel functions.[14–16] In the case of kinematic diffraction at given SAW amplitude, extinction of diffraction satellites can be observed (Fig. 3(a)). In the case of PSAW propagation, no suppression of the zero order diffraction satellite occurs, with the intensity of this diffraction satellite much exceeding the intensity of other diffraction satellites. The analysis of the rocking curves shows that PSAW is a flowing-back acoustic wave directed to the crystal depth. In the case of diffraction on PSAW, the X-ray radiation first diffracts on the near-surface non-modulated crystal lattice and then diffracts on deeper PSAW-modulated layers of the crystal lattice. This results in that the intensity of the zero diffraction satellite exceeds the diffracted intensities of the rest orders. In this case the X-ray diffraction on the LGT crystal is of dynamic character.

Figure 4 presents the dependences of diffraction satellite intensities on the amplitude of the input signal to the IDT for SAW (a) and PSAW (b). The character of the dependences is similar for SAW and PSAW. As the amplitudes of SAW and PSAW increase, the intensity of the zero diffraction satellite decreases. The intensities of the first diffraction satellites first increase with increasing of the amplitude of acoustic wave, reach a maximum at the amplitude of the input signal on the IDT $U = 12$ V, and then begin to decrease. It is clearly seen in Fig. 4 that in the case of PSAW in the LGT crystal the
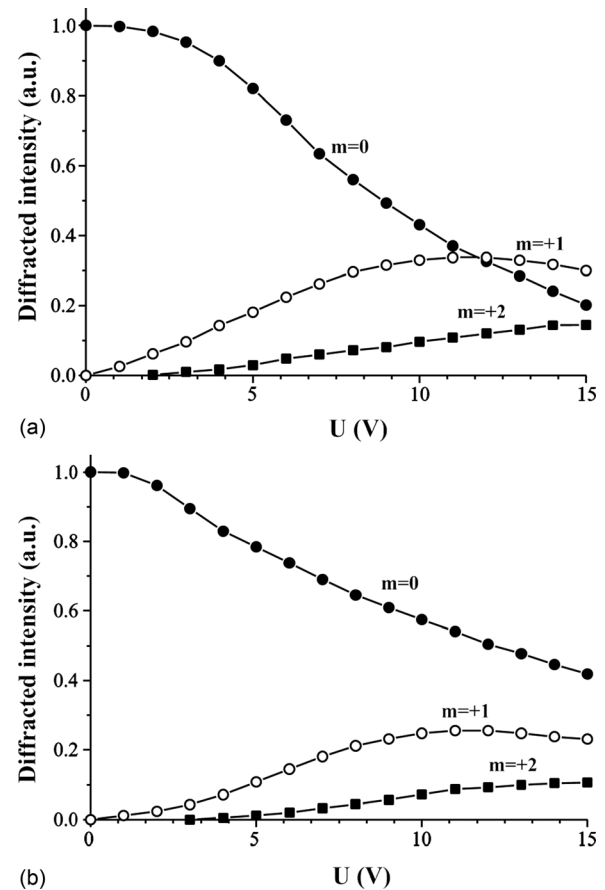
intensity of the zero diffraction satellites exceeds the intensity of the rest diffraction satellites because PSAW is excited by the IDT and tends to crystal depth at an angle to the surface.

V. CONCLUSION

X-ray diffraction on SAW and PSAW in the $Z-$cut of the LGT crystal was studied for the first time. The analysis of the diffraction spectra enabled the determination of the propagation velocities and power flow angles of the SAW and PSAW. It was shown that the velocity of PSAW exceeds that of SAW and the power flow angles of SAW and PSAW are of different values and signs. It was also found that SAW and PSAW are excited by the IDT, although at different resonance frequencies. The Rayleigh SAW was found to propagate in the crystal subsurface whereas the PSAW propagates from the IDT towards the crystal depth at an angle to the crystal surface. Figure 5 exhibits schematically the cross-section of the LGT crystal, the SAW (a) and PSAW (b) propagation, and X-ray diffraction on SAW and PSAW. In the case of PSAW, the X-ray radiation first diffracts on the crystal subsurface non-modulated by the acoustic wave and then part of the penetrated radiation diffracts deeper on the crystal lattice modulated by PSAW (Fig. 5(b)). This sequence of diffraction processes leads to a greater intensity of the zero diffraction satellite.
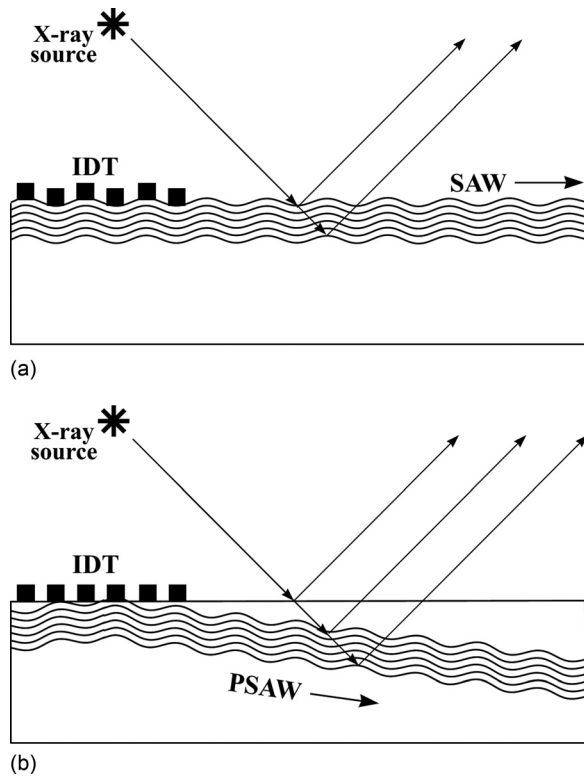
FIG. 5. Schemes of SAW (a) and PSAW (b) propagation in the Z−cut of a LGT crystal.

The difference in the power flow angles of SAW and PSAW looks promising from the viewpoint of creation of multifunctional multifrequency acoustoelectronic devices which can operate in various frequency ranges using one source of generation of various acoustic waves (e.g., an inter-digital transducer).

Further development of the X-ray diffraction model and employment of the X-ray diffraction on a PSAW modulated crystal would enable the angle between the crystal surface and PSAW propagation direction to be determined.

[1]M. P. du Cunda and S. A. Fagundes, IEEE Trans. Ultrason. Ferroelectr. Freq. Control **46**, 1583 (1999).

[2]R. C. Smythe, R. C. Helmbold, G. E. Hague, and K. A. Snow, IEEE Trans. Ultrason. Ferroelectr. Freq. Control **47**, 355 (2000).

[3]H. Fritze and H. L. Tuller, Appl. Phys. Lett **78**, 976 (2001).

[4]N. Naumenko, IEEE Trans. Ultrason. Ferroelectr. Freq. Control **48**, 530(2001).

[5]H. Cerva and W. Graeff, Phys. Status Solidi A **82**, 35 (1984).

[6]R. W. Whatmore, P. A. Goddard, B. K. Tanner, and G. F. Clark, Nature **299**, 44 (1982).

[7]E. Zolotoyabko, D. Shilo, W. Sauer, E. Pernot, and J. Baruchel, Appl. Phys. Lett. **73**, 2278 (1998).

[8]D. Shilo and E. Zolotoyabko, J. Phys. D: Appl. Phys. **36**, A122 (2003).

[9]D. V. Roshchupkin, H. D. Roshchupkina, and D. V. Irzhak, IEEE Trans. Ultrason. Ferroelectr. Freq. Control **52**, 2081 (2005).

[10]D. V. Irzhak, D. V. Roshchupkin, D. V. Punegov, and S. A. Sakharov, Bull. Russ. Acad. Sci. Phys. **71**, 72 (2007).

[11]W. Sauer, T. H. Metzger, A. G. C. Haubrich, S. Manus, A. Wixforth, J. Peisl, A. Mazuelas, J. Härtwig, and J. Baruchel, Appl. Phys. Lett. **75**, 1709 (1999).

[12]R. Tucoulou, R. Pascal, M. Brunel, O. Mathon, D. V. Roshchupkin, I. A. Schelokov, E. Cattan, and D. Remeins, J. Appl. Crystallogr. **33**, 1019 (2000).

[13]R. Tucoulou, F. de Bergevin, O. Mathon, and D. V. Roshchupkin, Phys. Rev. B **64**, 134108 (2001).

[14]D. V. Roshchupkin, D. V. Irzhak, R. Tucoulou, and O. A. Buzanov, J. Appl. Phys. **94**, 6692 (2003).

[15]D. V. Roshchupkin, A. I. Erko, L. Ortega, and D. V. Irzhak, Appl. Phys. A **94**, 477 (2009).

[16]D. Roshchupkin, D. Irzhak, A. Snigirev, I. Snigireva, L. Ortega, and A. Sergeev, J. Appl. Phys. **110**, 124902 (2011).

[17]S. Sakharov, D. Roshchupkin, E. Emelin, D. Irzhak, O. Buzanov, and A. Zabelin, Procedia Eng. **25**, 1020 (2011).

[18]J. Bohm, E. Chilla, H.-J. Fröhlich, T. Hauke, R. B. Heimann, and U. Straube, J. Cryst. Growth **216**, 293 (2000).